

**Molecular Cell, Volume 83**

**Supplemental information**

**Visualization of direct and diffusion-assisted**

**RAD51 nucleation by full-length**

**human BRCA2 protein**

**Ondrej Belan, Luke Greenhough, Lucas Kuhlen, Roopesh Anand, Artur Kaczmarczyk, Dominika T. Gruszka, Hasan Yardimci, Xiaodong Zhang, David S. Rueda, Stephen C. West, and Simon J. Boulton**

## Supplementary Figures

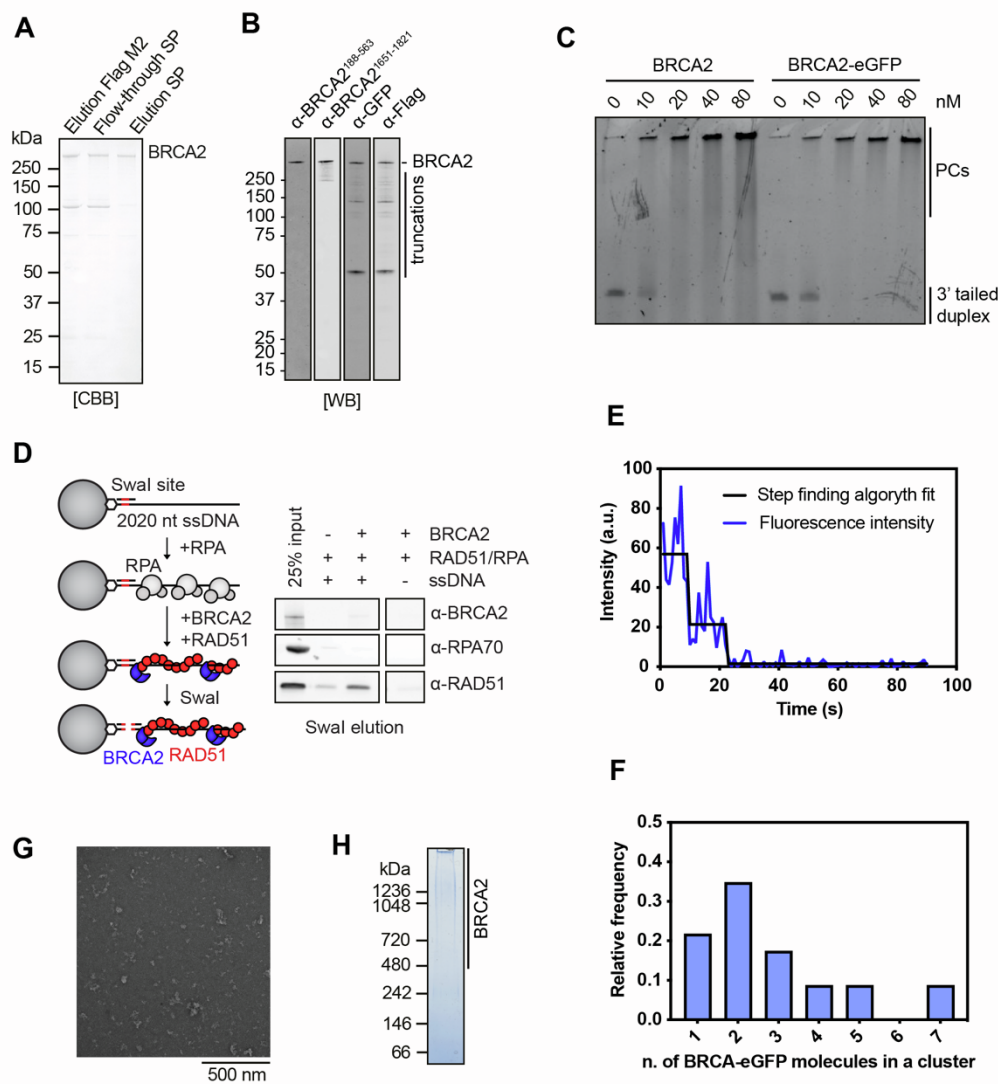


**Figure S1: BRCA2 characterization. Related to Fig. 1.** (A) Purification of full-length human BRCA2. (B) Western blot of purified BRCA2-eGFP performed using antibodies targeting indicated epitopes (N-terminal and central region of BRCA2; eGFP; FLAG). (C) Electrophoretic mobility shift assay (EMSA) performed with 167mer 3' tailed DNA and BRCA2 or BRCA2-eGFP. PCs - protein-DNA complexes. (D) DNA capture assay. Biotinylated RPA-coated 2020 nt-long ssDNA immobilized on streptavidin-coated beads was incubated with RAD51 and BRCA2, washed and proteins were eluted via Swal cleavage of the DNA. Samples were analysed by SDS-PAGE. Quantitative analysis was performed following western-blotting and fluorescent detection using Licor system. (E) Examples of a fluorescence intensity trace of the BRCA2-eGFP cluster during continuous photobleaching. Black line represents stepping fit of the trace. (F) Histogram of BRCA2 cluster size in the presence of RAD51 (N = 23 molecules). (G) Electron micrograph of recombinant BRCA2 negatively stained with uranyl acetate. The sample is polydisperse owing to the range of oligomeric states observed. (H) 3-12% Native PAGE of recombinant BRCA2, stained with Coomassie.

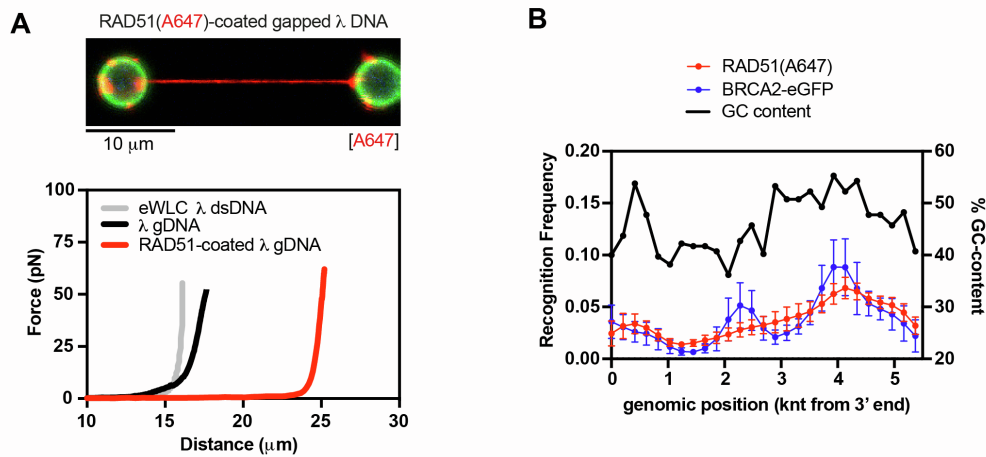


**Figure S2: RAD51-gDNA characterization and further nucleation position-sequence analysis. Related to Fig. 2 and Fig. 3. (A)** Top: representative image of RAD51(A647)-coated  $\lambda$  gDNA held at  $\sim 5$  pN force. Bottom: force extension curves of  $\lambda$  gDNA (with 5.374 knt-long ssDNA gap, black), force extension curves of  $\lambda$  gDNA coated with RAD51(A647) (red). Gray line represents extensible worm-like chain model (eWLC) for 48.5 kb  $\lambda$  dsDNA as a reference. **(B)** Position analysis of RAD51(A647) (red) or BRCA2-eGFP (blue) binding along the length of 5.374 knt ssDNA gap in the absence of RPA.  $N = 6$  molecules. Error bars represent S.E.M. 200 nt bins. GC-content of the DNA sequence within each bin is indicated in black.

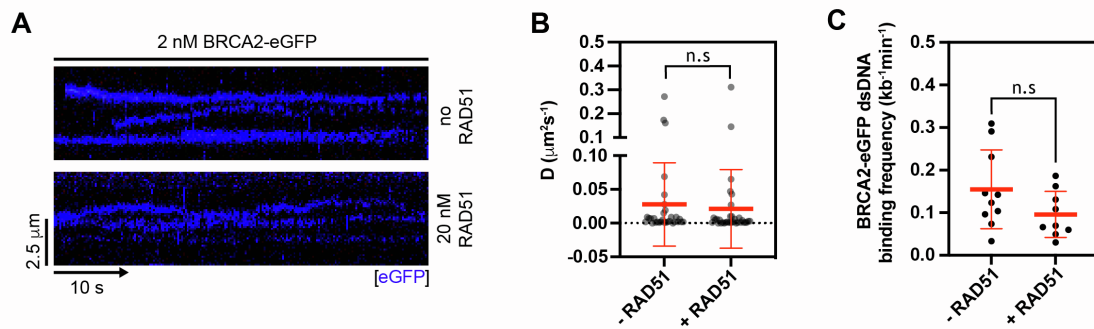


**Figure S3: BRCA2 diffusion on dsDNA in the absence of RAD51. Related to Fig. 4. (A)** Representative kymographs demonstrating diffusion of BRCA2-eGFP (blue) along  $\lambda$  dsDNA at 10 pN in the presence of 50 mM NaCl, 2 mM  $\text{MgCl}_2$  and 2 mM ATP in the presence or absence of 20 nM RAD51 (unlabelled). **(B)** Diffusion coefficient ( $D$ ) calculated from MSD analysis for BRCA2-eGFP complexes moving on dsDNA in the presence or absence of RAD51. Lines represent mean. Error bars represent S.D. P values by Mann-Whitney test. (n.s.)  $P > 0.05$ ; (\*)  $P \leq 0.05$ ; (\*\*)  $P \leq 0.01$ ; (\*\*\*)  $P \leq 0.001$ ; (\*\*\*\*)  $P \leq 0.0001$ . **(C)** dsDNA binding frequency of BRCA2-eGFP in the presence or absence of 20 nM RAD51, 50 mM NaCl, 2 mM  $\text{MgCl}_2$ , 2 mM ATP on dsDNA held at 10 pN force. Lines represent mean. Error bars represent S.D. P values by student t test.

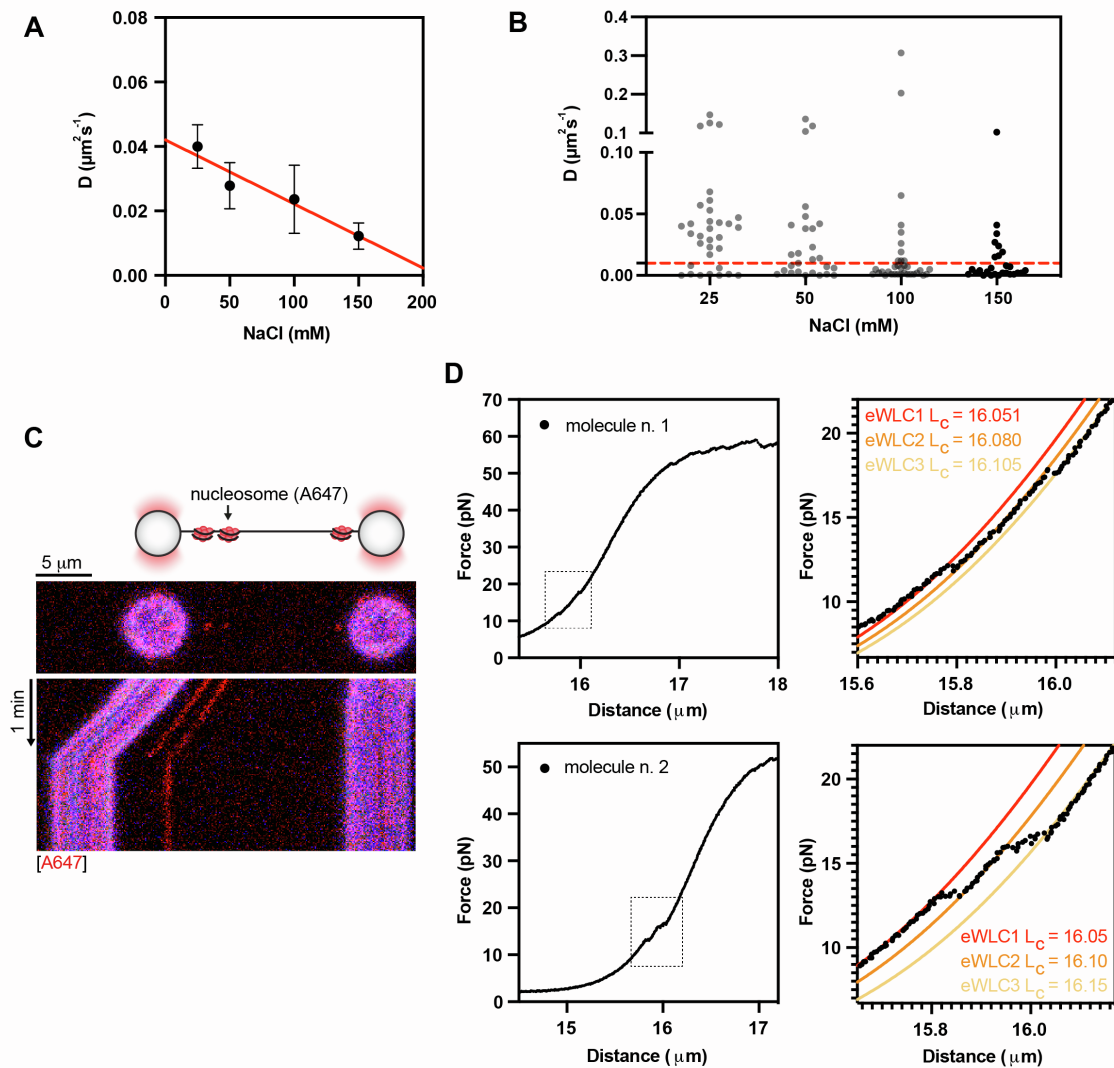


**Figure S4: Characterization of chromatinized  $\lambda$  DNA. Related to Fig. 5. (A)** Diffusion coefficient ( $N = 27\text{-}34$ ) calculated for BRCA2-RAD51 complexes as a function of salt concentration. Error bars represent S.E.M. **(B)** Diffusion coefficient distribution calculated for BRCA2-RAD51 complexes at different salt concentrations. Red dashed line represents static fraction cut-off. **(C)** Representative kymograph showing stretching of sparsely chromatinized  $\lambda$  DNA. Alexa Fluor 647-labelled nucleosomes are shown in red. **(D)** Two examples of force-distance curve of sparsely chromatinized  $\lambda$  DNA. Individual unwrapping events characterized by sudden distance increase under the same force are highlighted in a dashed line box. Lines correspond to extensible worm-like chain (eWLC) models of dsDNA aligned with the corresponding force-extension curve segments.  $L_c$  corresponds to calculated contour length of DNA from the fit.  $L_c$  difference between adjacent eWLCs corresponds to length of DNA released during a nucleosome unwrapping event.

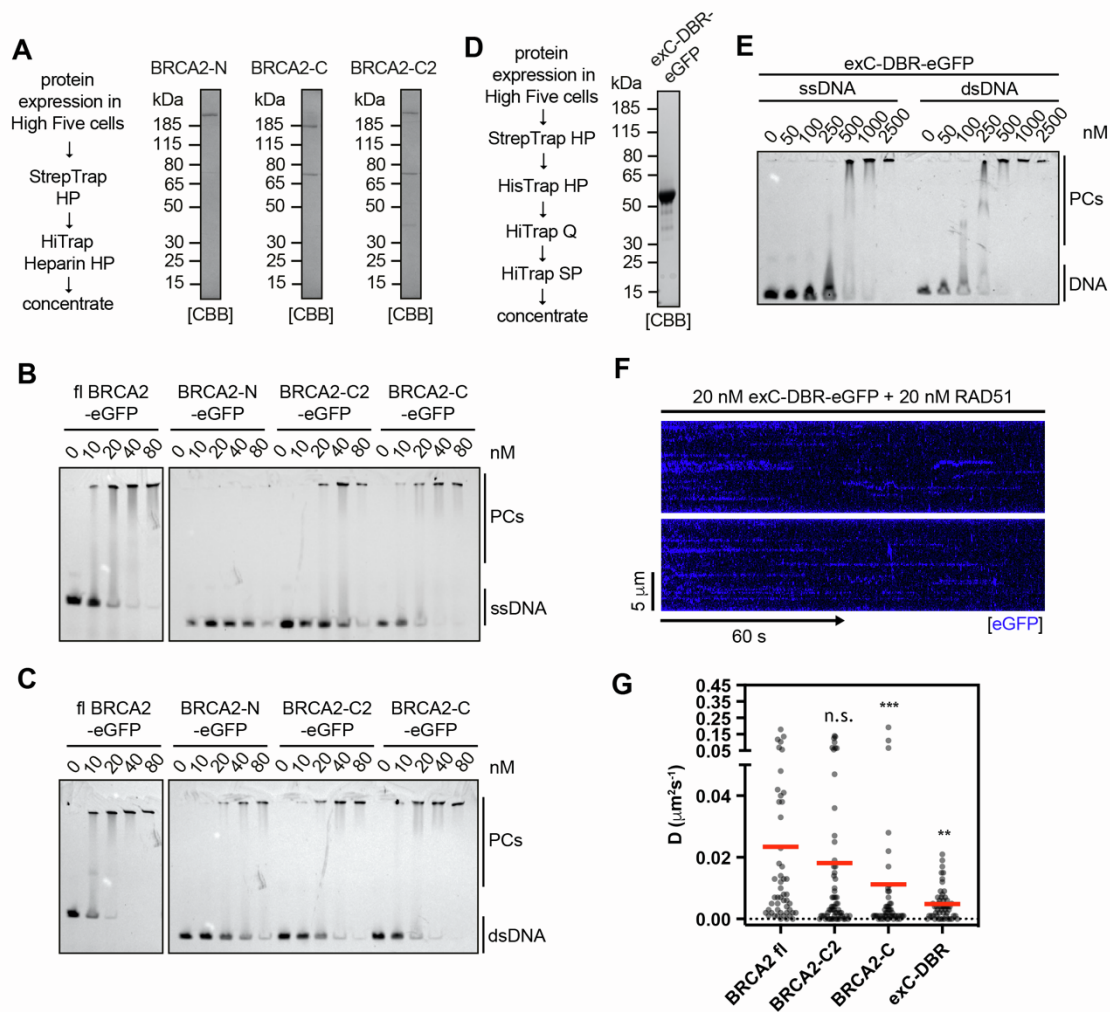


**Figure S5: Further characterization of BRCA2 mutants. Related to Fig. 6. (A)** Purification of BRCA2-N, BRCA2-C and BRCA2-C2 truncation mutants. Proteins were resolved by SDS-PAGE and stained by Coomassie Brilliant Blue staining (CBB). **(B)** Electrophoretic mobility shift assay (EMSA) to assess affinity of BRCA2 and BRCA2 truncation mutants to 100mer ssDNA. **(C)** Electrophoretic mobility shift assay (EMSA) to assess affinity of BRCA2 and BRCA2 truncation mutants to 100mer dsDNA. PCs - protein-DNA complexes. **(D)** Purification of exC-DBR-eGFP fusion. Protein resolved by SDS-PAGE and stained by Coomassie Brilliant Blue staining (CBB). **(E)** Electrophoretic mobility shift assay (EMSA) to assess affinity of exC-DBR-eGFP to 100mer ss- and dsDNA. PCs - protein-DNA complexes. **(F)** Two representative kymographs demonstrating limited diffusion of exC-DBR-eGFP (blue) along  $\lambda$  dsDNA at 10 pN in the presence of 50 mM NaCl, 2 mM MgCl<sub>2</sub>, 2 mM ATP and 20 nM RAD51 (unlabelled). **(G)** Diffusion coefficient (D) calculated from MSD analysis for exC-DBR-eGFP molecules moving on dsDNA in the presence of RAD51. Lines represent mean. Data for BRCA2 fl, BRCA2-C and BRCA2-C2 are of the same dataset as in Fig. 6H. P values by Mann-Whitney test. (n.s.) P > 0.05; (\*) P  $\leq$  0.05; (\*\*) P  $\leq$  0.01; (\*\*\*) P  $\leq$  0.001; (\*\*\*\*) P  $\leq$  0.0001.

Oligonucleotides		
Oligonucleotide name and sequence	Source	Identifier
100mer ssDNA 5'-Cy5- CCAAGAAGCTGTTCAAGAATCAGAATGAGCCGCAACT CGGGATGAAAATGCTCACAATGACAAA- TCTGTCCACGGAGTGCTTAATCCAACCTACCAAGCT-3'	IDT, this study	N/A
100mer dsDNA bottom 5'- AGCTTGTAAGTTGGATTAAGCACTCCGTGGACAGAT TTGTCATTGTGAGCATTTCATCCCGAAGTTGCGGCTC ATTCTGATTCTGAACAGCTTCTTGG-3'	IDT, this study	N/A
3'tailed DNA top 5'-Cy5- CTGCTTTATCAAGATAATTTTTCGACTCATCAGAAATA TCCGTTTCCTATATTTATTCCTATTA- TGTTTTATTCACTTACTTATTCTTTATGTTCATTTTTAT ATCCTTACTTTATTTCTCTGTTTATTCATTTACTTATT TTGTATTATCCTTATCTTATTTA-3'	IDT, this study	N/A
3'tailed DNA bottom 5'-CGGATATTTCTGATGAGTCGAAAAATTATCTTGA- TAAAGCAG-3'	IDT, this study	N/A
biot-Swal-2023bp-f 5'-biotin- AACAAAATATTAACGCTTACAATTTAAATGGTGGCAC TTTTCG-3'	IDT, this study	N/A
2023bp-r 5'-TCAACGTGCAATCAAGTTAATGAATCGG-3'	IDT, this study	N/A
biot-Swal-rc 5'- CGAAAAGTGCCACCATTTAAATTGTAAGCGTTAATAT TTTGTT-3'	IDT, this study	N/A
λ DNA end-cap 1 5'- AGGTCGCCGCCCGGAGTTGAACG(BT)(BT)T(BT)T(BT) ACGTTCAACTCC-3'	IDT, Belan et al, 2021	N/A
λ DNA end-cap 2 5'-GGGCGGCGCA CCTCAAGTTGGACAA(BT)T(BT)T(BT)(BT)TGTCCTCAACT TG-3'	IDT, Belan et al, 2021	N/A
λ DNA handles oligo 1 5'-GGGCGGCGACCTGGACAA-3'	Sigma Aldrich, Belan et al, 2021	N/A
λ DNA handles oligo 2 5'-AGGTCGCCGCCCTTTTTTTT(BT)TT(BT)TT(BT)-3'	Sigma Aldrich, Belan et al, 2021	N/A

<p>λ DNA handles oligo 3  5'-  T(BT)TT(BT)TT(BT)TTTTTTAGAGTACTGTACGATCTA  GCATCAATCTTGTCC-3')</p>	<p>Sigma Aldrich, Belan  et al, 2021</p>	<p>N/A</p>
<p>crRNA λ4  5'-CAGAUAUAGCCUGGUGGUUCGUUUUAGAGC  UAUGCUGUUUUG-3'</p>	<p>IDT, Belan et al, 2021</p>	<p>N/A</p>
<p>crRNA λ5  5'-  GGCAAUGCCGAUGGCGAUAGGUUUUAGAGCUAUG  CUGUUUUG-3'</p>	<p>IDT, Belan et al, 2021</p>	<p>N/A</p>
<p>tracr RNA (trRNA)  5'-GGACAGCAUAGCAAGU  UAAAAUAAGGCUAGUCCGUUAUCAACUUGAAA  AAGUGGCACCGAGUCGGUGCUUUUU-3'</p>	<p>IDT, Belan et al, 2021</p>	<p>N/A</p>

**Table S1: Oligonucleotides used in the study.** Related to KEY RESOURCE TABLE.